Supporting Information

For

Insight into the reversible behavior of Lewis-Brønsted basic poly(ionic liquid)s in one-pot two-step chemical fixation of CO_2 to linear carbonate

*Yuting He[a], Huimin Lu[a], Xue Li[a], Jun Wu[a], Tiancheng Pu[c], Wei Du[a], Hongping Li[b], Jing Ding[*a], Hui Wan[a], Guofeng Guan[*a]*

[a] State Key Laboratory of Materials-Oriented Chemical Engineering, College of Chemical Engineering, Jiangsu National Synergetic Innovation Center for Advanced Materials, Nanjing Tech University, Nanjing 210009, PR China.

[b] Institute for Energy Research of Jiangsu University, Jiangsu University, Jiangsu 212013, PR China.

[c] State Key Laboratory of Chemical Engineering, East China University of Science and Technology, Shanghai 200237, PR China.

* Corresponding authors

E-mails: jding@njtech.edu.cn (Jing Ding)

guangf@njtech.edu.cn (Guofeng Guan)

Tel: +86 25 83587198, Fax: +86 25 83587198

Catalyst characterization

^{1}H NMR spectra and ^{13}C NMR spectra were performed on a Bruker DPX 500 spectrometer at ambient temperature by using D_2O as the deuterium reagent. Fourier transform infrared (FT-IR) spectra were determined on a Thermo Nicolet 6700 spectrometer in the wavenumber range of 4000-500 cm^{-1} of fully dried samples mixed with KBr. X-ray photoelectron spectroscopy (XPS) was conducted on a PHI 5000 Versa Probe X-ray photoelectron spectrometer equipped with Al Kα radiation (1486.6 eV) as the X-ray source. The C 1s peak at 284.5 eV was used as the reference for the binding energies. Brunauer-Emmett-Teller (BET) surface areas, pore volumes and pore-size distributions of the samples were calculated from nitrogen adsorption–desorption isotherms acquired on a BELSORP-MINI instrument at 77 K. Scanning electron microscopy (SEM) images were investigated on a Regulus 8220 scanning electron microscope (10 kV). Thermal gravimetric (TG) analysis experiments were carried out with a STA409 instrument under the N_2 flow at a heating rate of 10 $K \cdot min^{-1}$. An FT-IR spectrometer (PerkinElmer Frontier) equipped with an *in situ* diffuse reflection cell (Harrick Praying Mantis) was used for *in situ* DRIFTS analysis.

Computational details

Density functional theory (DFT) calculations based on quantum mechanics were carried out with Gaussian 09 suite of programs. The geometric optimization of the structures and frequency analysis were carried out by using the B3LYP functional with the 6-311++G** basis set with empirical dispersion. Non-covalent interaction (NCI) and electrostatic potential (ESP) [1] were analyzed by Multiwfn 3.8 (wave function analysis) [2] and VMD 1.9.2 (molecular visualization) [3], respectively.

Synthesis of amino-derived ILs monomer [VBTEDA]Cl

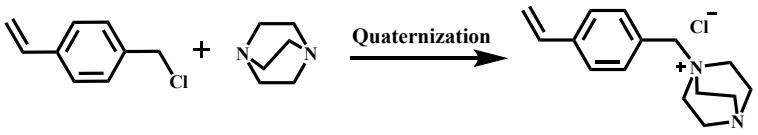

Synthesis of carboxyl-derived ILs monomer [CEVIm]Cl

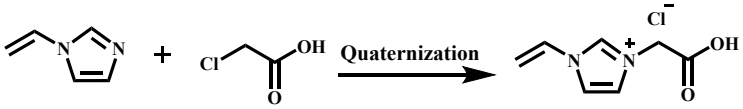

Scheme S1. Synthetic procedure of functionalized ILs monomer.

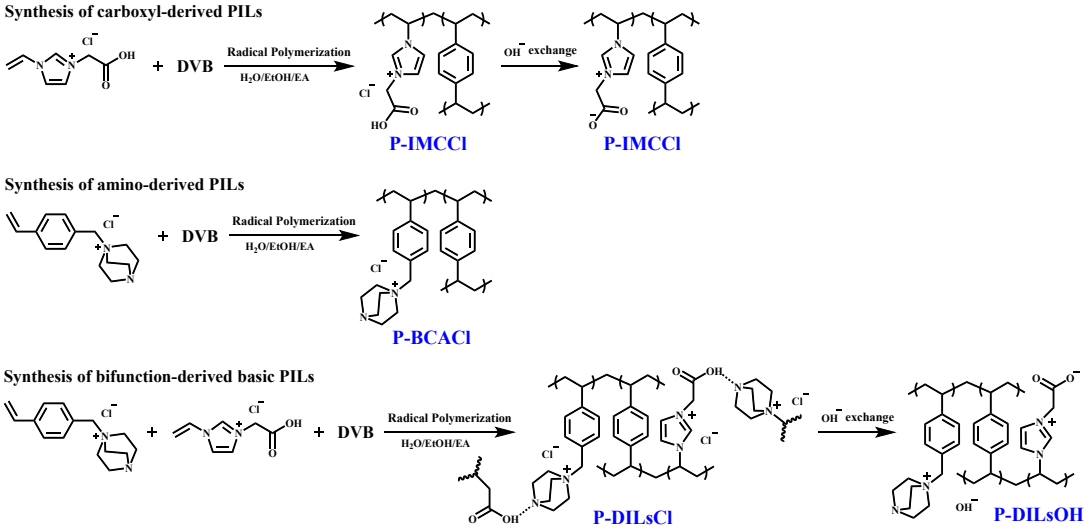

Scheme S2. Synthetic procedure of functionalized PILs.

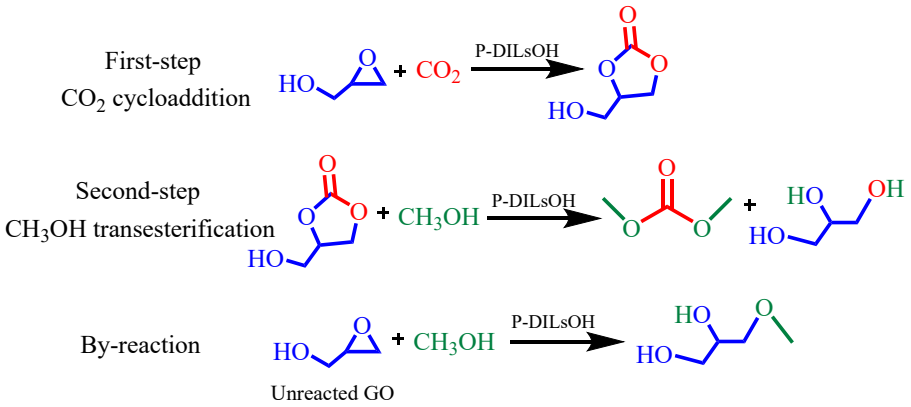

Scheme S3. Catalytic procedure of two-step synthesis method.

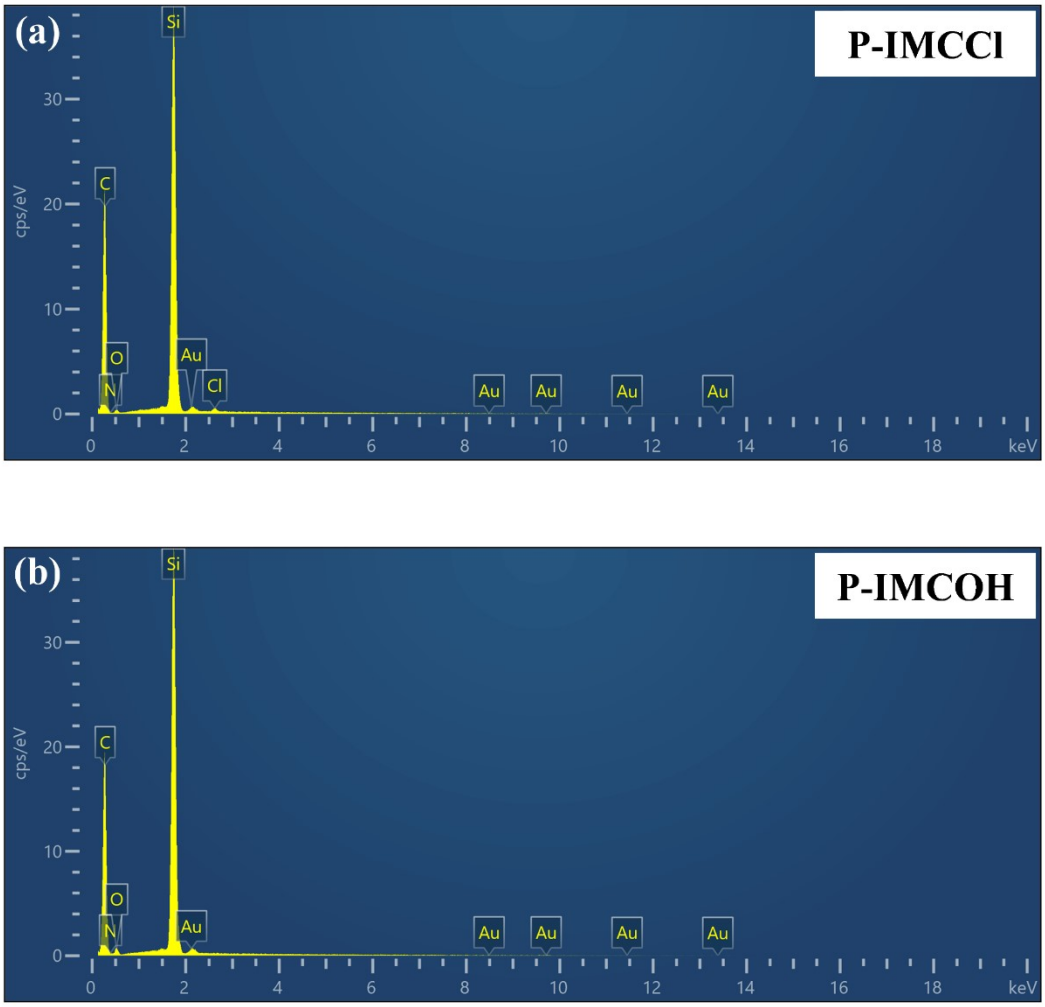

Fig. S1. EDS spectra of (a) P-IMCCl and (b) P-IMC (the sample was coated on polished silicon wafers and sprayed with gold for 90 s).

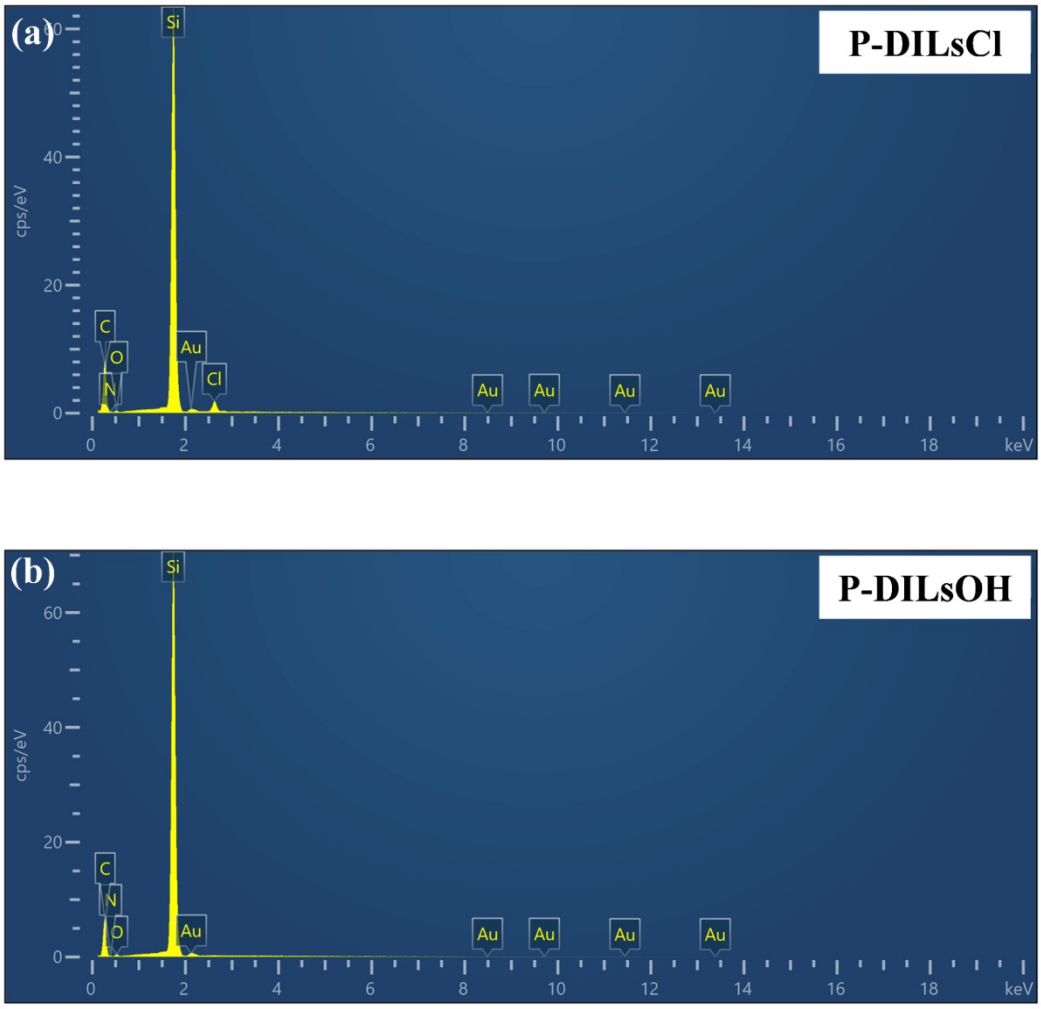

Fig. S2. EDS spectra of (a) P-DILsCl and (b) DILsOH (the sample was coated on polished silicon wafers and sprayed with gold for 90 s).

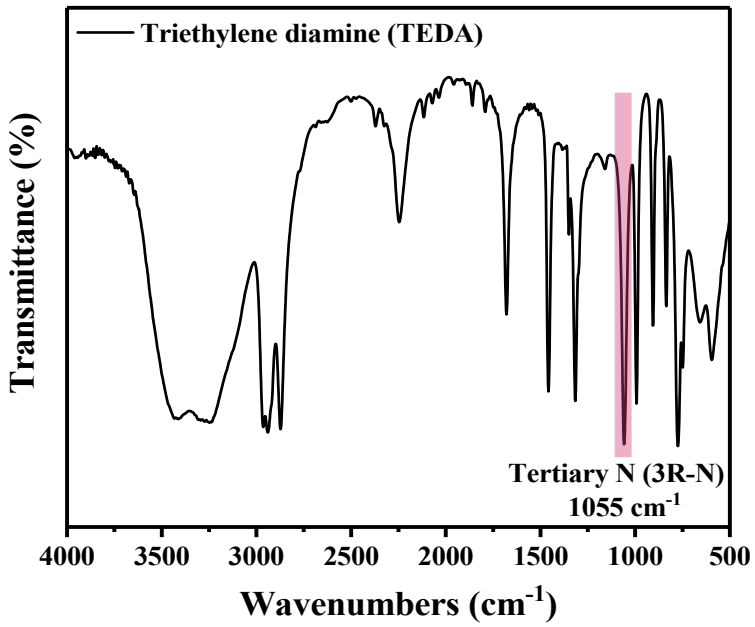

Fig. S3. FT-IR spectra of Triethylene diamine.

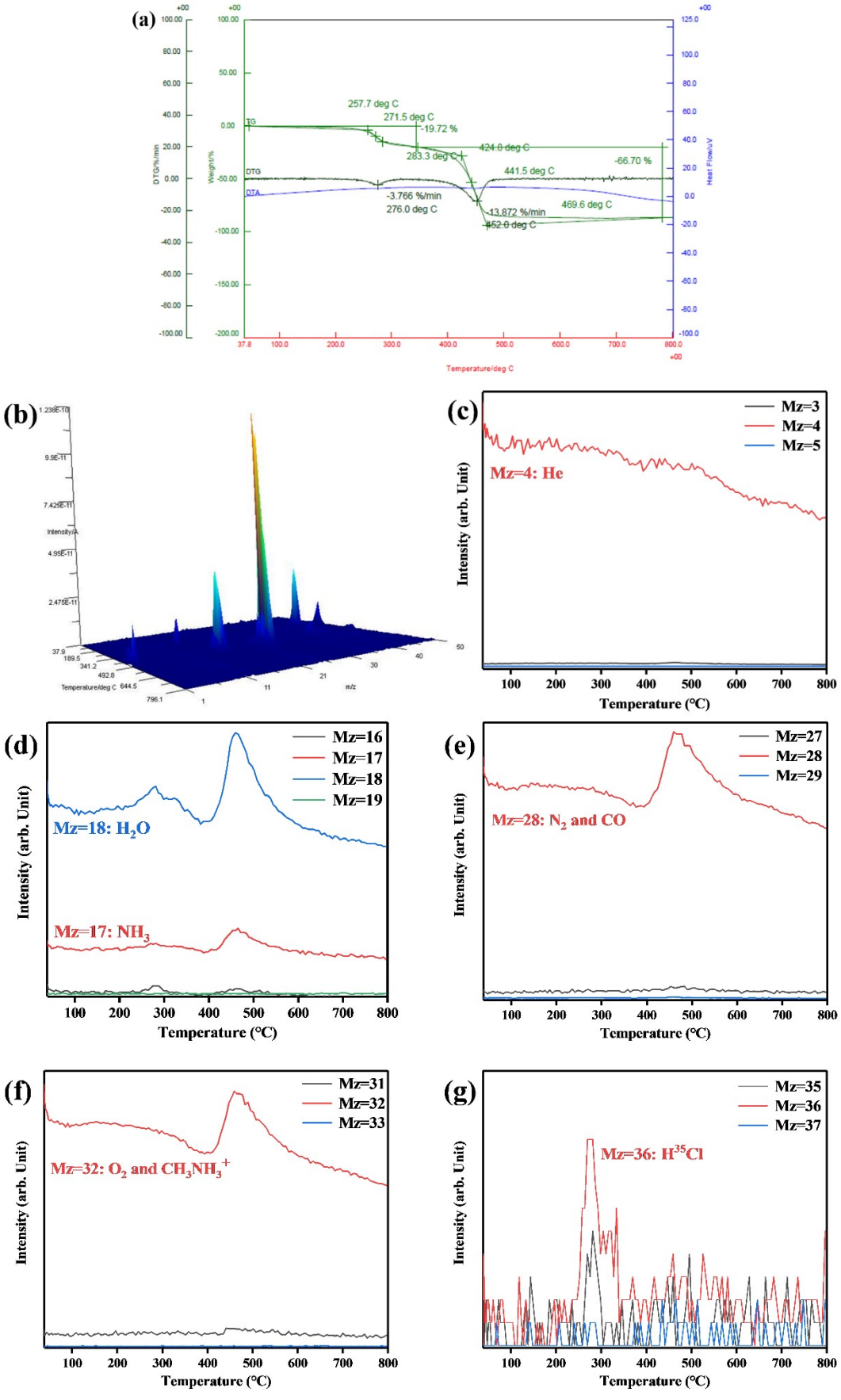
(a)
257.7 deg C
271.5 deg C
-19.72 %
283.3 deg C
424.6 deg C
-66.70 %
441.5 deg C
469.6 deg C
-3.766 %/min
276.0 deg C
-13.872 %/min
452.0 deg C
TG
DTG
DTA
Temperature/deg C
(b)
Intensity/A
Temperature/deg C
m/z
(c)
Mz=3
Mz=4
Mz=5
Mz=4: He
Intensity (arb. Unit)
Temperature (°C)
(d)
Mz=16
Mz=17
Mz=18
Mz=19
Mz=18: H2O
Mz=17: NH3
Intensity (arb. Unit)
Temperature (°C)
(e)
Mz=27
Mz=28
Mz=29
Mz=28: N2 and CO
Intensity (arb. Unit)
Temperature (°C)
(f)
Mz=31
Mz=32
Mz=33
Mz=32: O2 and CH3NH3+
Intensity (arb. Unit)
Temperature (°C)
(g)
Mz=35
Mz=36
Mz=37
Mz=36: H35Cl
Intensity (arb. Unit)
Temperature (°C)

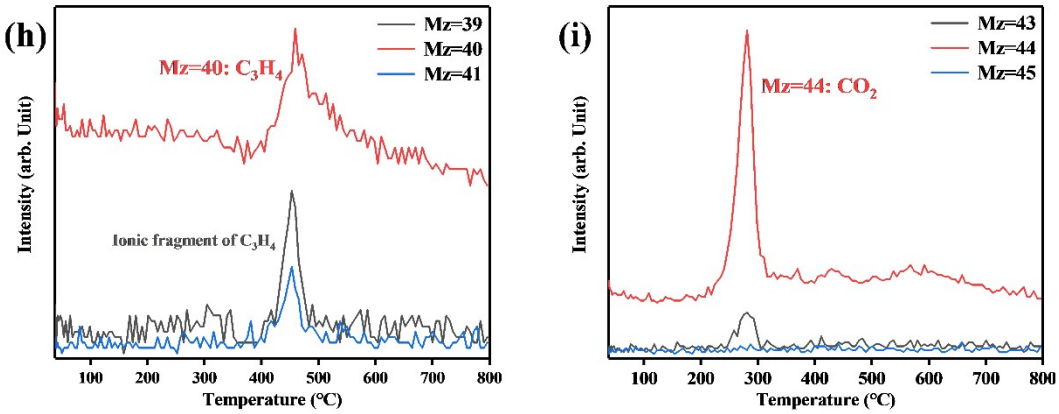

Fig. S4. TG-Mass result of P-DILsCl. (a) TG, DTG and DTA curves of P-DILsCl. (b) Relationship between molecular weight of P-DILsCl pyrolysis products and signal intensity with pyrolysis temperature. (c-i) Relationship between different molecular weight pyrolysis products of signal intensity with pyrolysis temperature.

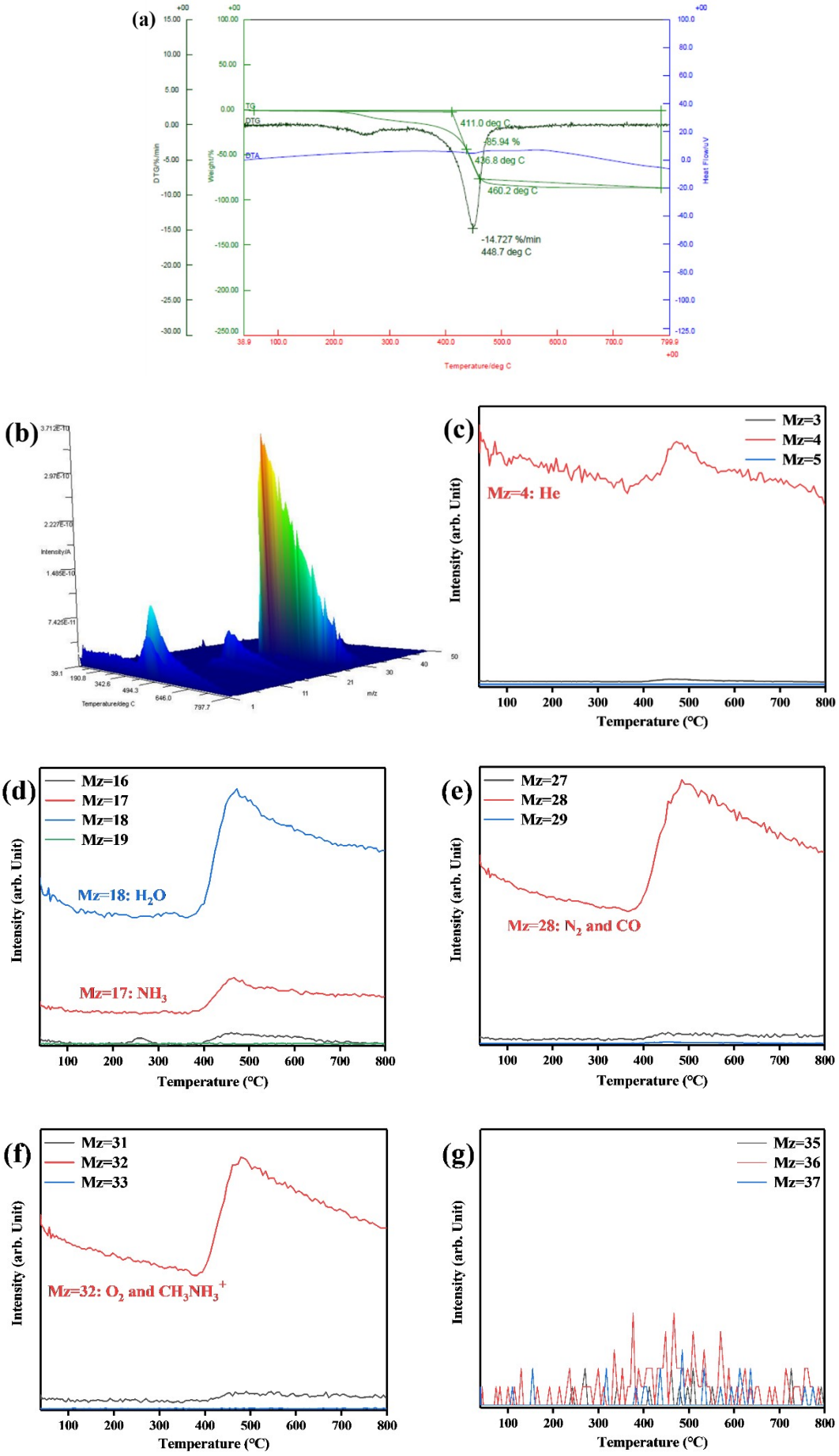
(a)
TG
DTG
DTA
411.0 deg C
-85.94 %
436.8 deg C
460.2 deg C
-14.727 %/min
448.7 deg C
Temperature/deg C
(b)
Intensity/A
Temperature/deg C
m/z
(c)
Mz=3
Mz=4
Mz=5
Mz=4: He
Intensity (arb. Unit)
Temperature (°C)
(d)
Mz=16
Mz=17
Mz=18
Mz=19
Mz=18: H2O
Mz=17: NH3
Intensity (arb. Unit)
Temperature (°C)
(e)
Mz=27
Mz=28
Mz=29
Mz=28: N2 and CO
Intensity (arb. Unit)
Temperature (°C)
(f)
Mz=31
Mz=32
Mz=33
Mz=32: O2 and CH3NH3+
Intensity (arb. Unit)
Temperature (°C)
(g)
Mz=35
Mz=36
Mz=37
Intensity (arb. Unit)
Temperature (°C)

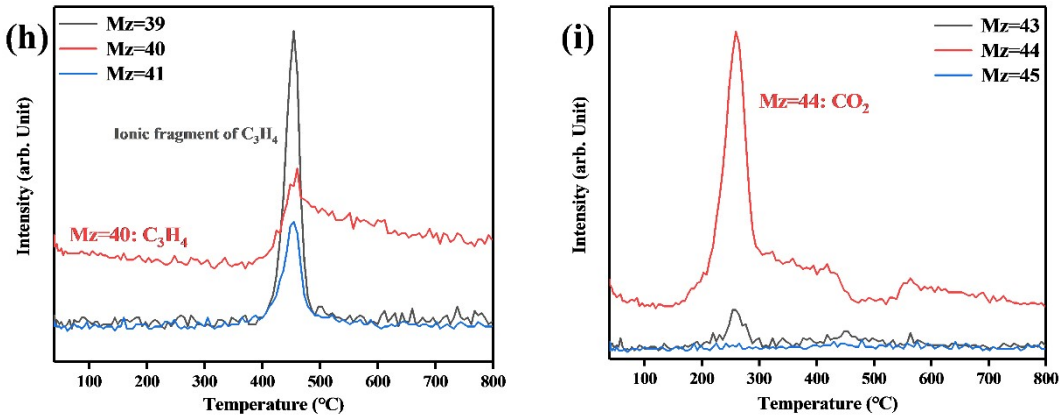

Fig. S5. TG-Mass result of P-DILsOH. (a) TG, DTG and DTA curves of P-DILsOH. (b) Relationship between molecular weight of P-DILsCl pyrolysis products and signal intensity with pyrolysis temperature. (c-i) Relationship between different molecular weight pyrolysis products of signal intensity with pyrolysis temperature.

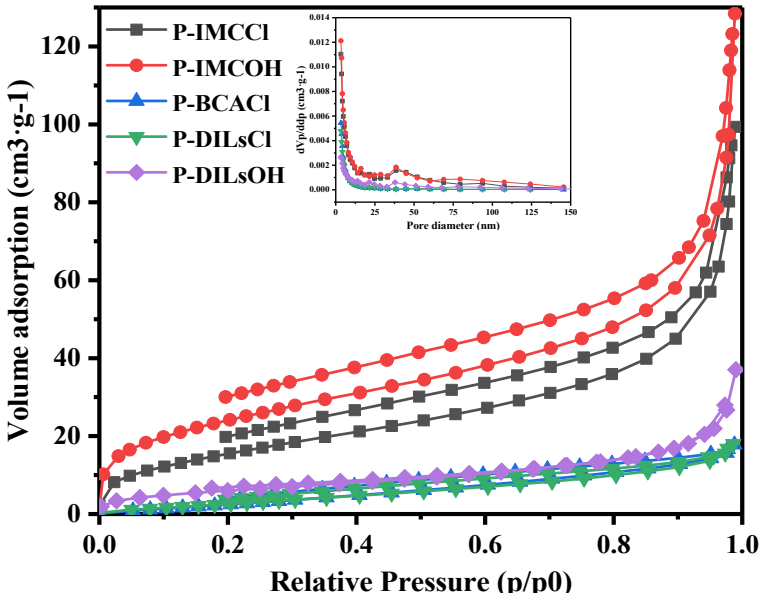

Fig. S6. N_2 sorption isotherms and pore size distribution curves.

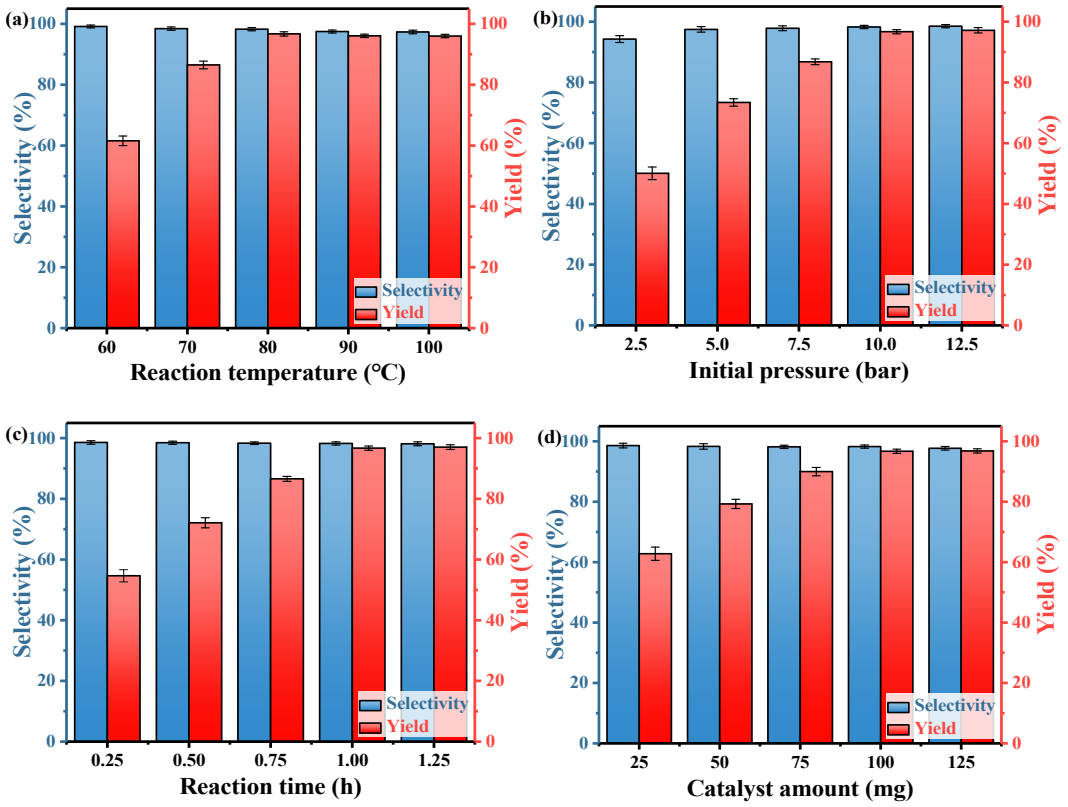

Fig. S7. Dependencies of GLC yields on different parameters over P-DILsOH in CO_2 cycloaddition. (a) the effect of reaction temperature (conditions: 10 bar CO_2, 1.0 h, 100 mg catalyst). (b) the effect of CO_2 pressure (conditions: 80 °C, 1.0 h, 100 mg catalyst). (c) the effect of reaction time (conditions: 80 °C, 10 bar CO_2, 100 mg catalyst). (d) the effect of catalyst amount (conditions: 80 °C, 10 bar CO_2, 1 h).

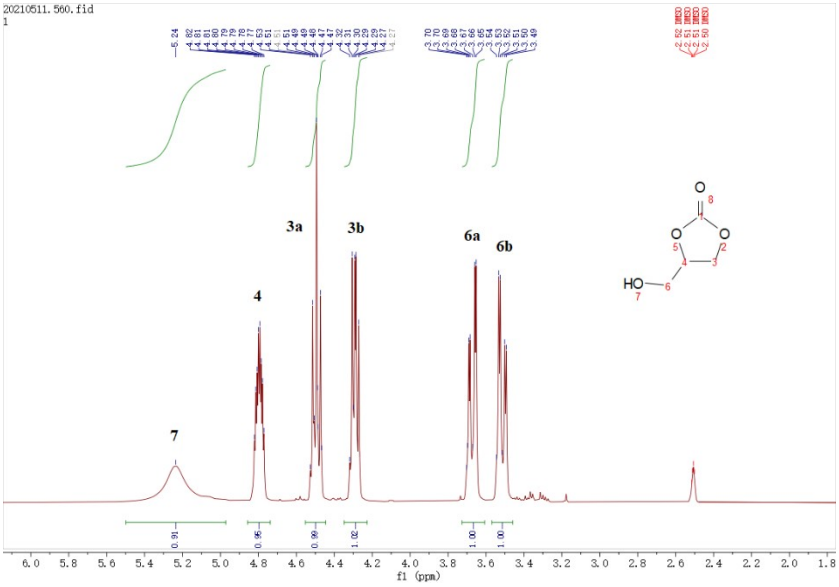

Fig. S8. ^{1}H NMR of products after the cycloaddition reaction.

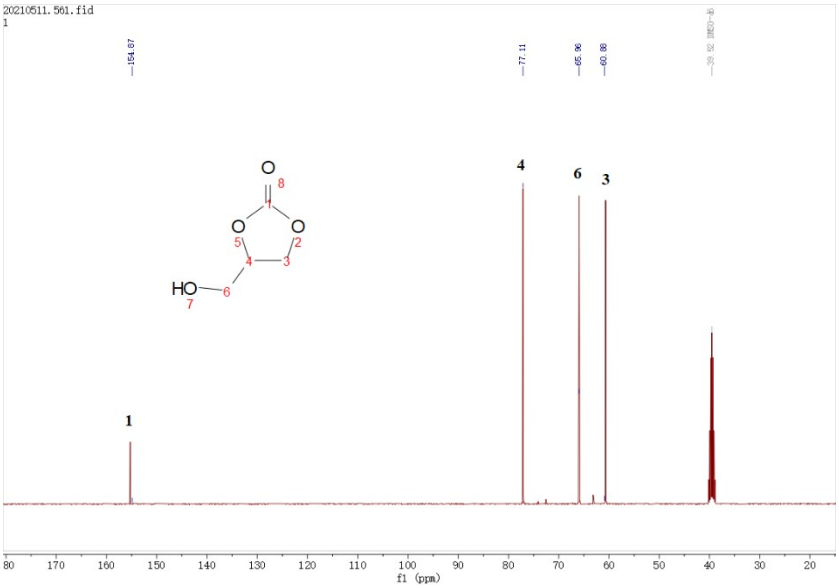

Fig. S9. ^{13}C NMR of products after the cycloaddition reaction.

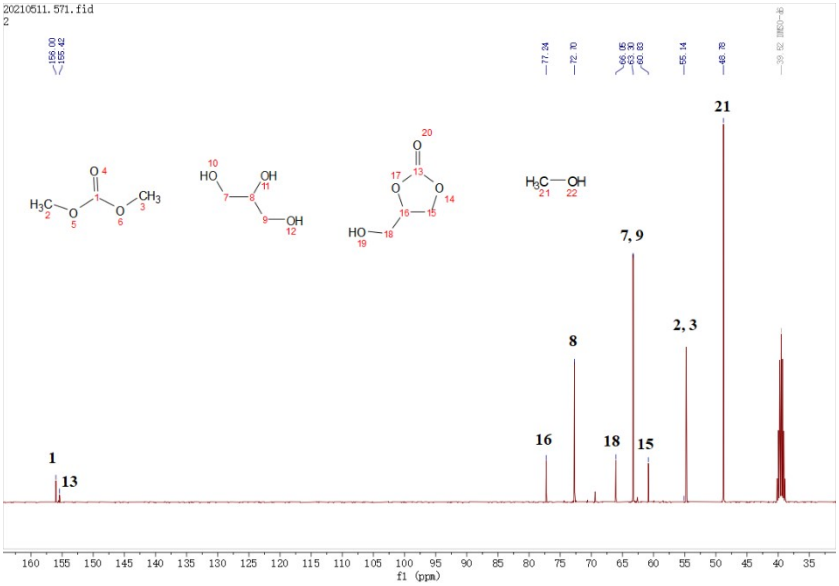

Fig. S10. ^{1}H NMR of products after the transesterification reaction.

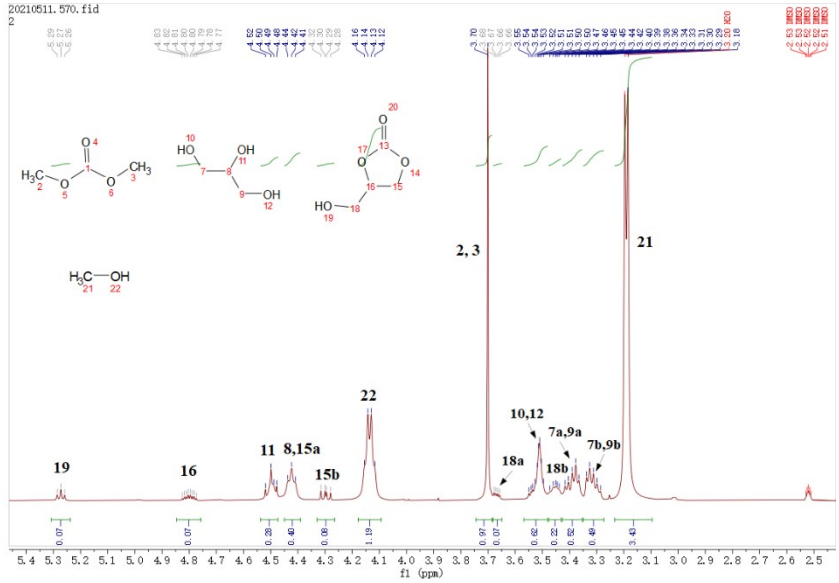

Fig. S11. ^{13}C NMR of products after the transesterification reaction.

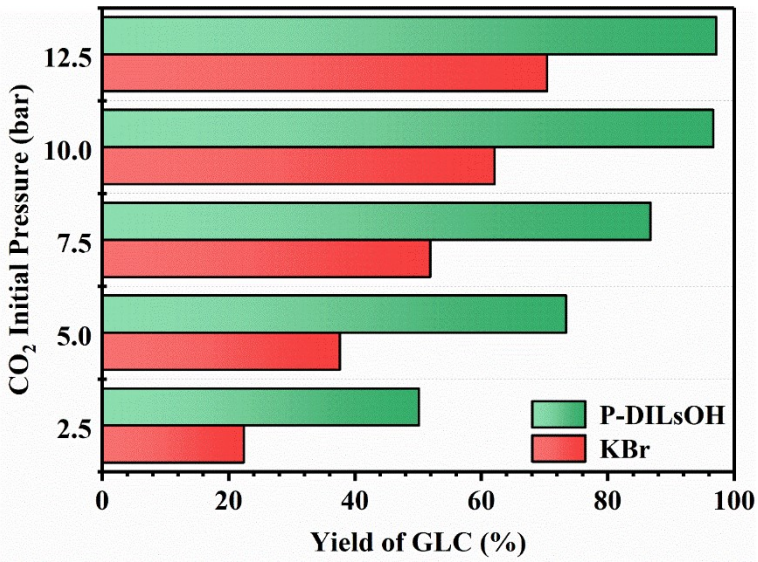

Fig. S12. Comparison of cycloaddition activities over P-DILsOH and KBr under different CO_2 pressures. Reaction conditions: GO (15 mmol), 80 °C, 1 h, catalysts (100 mg).

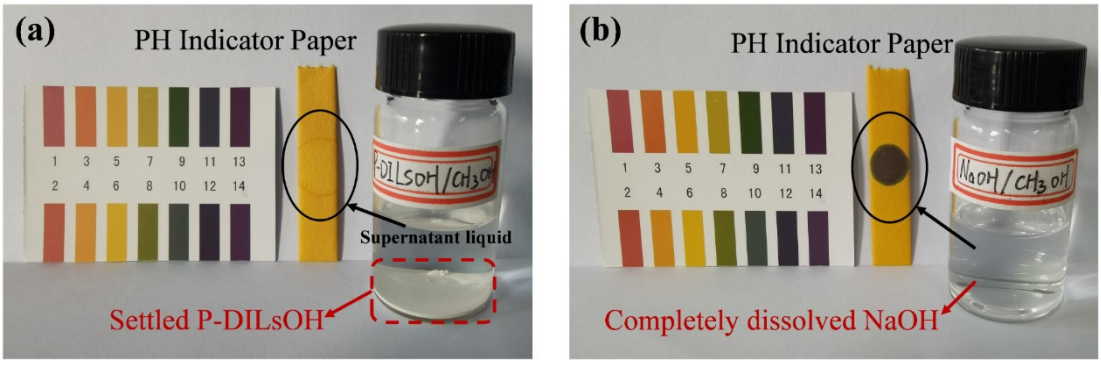

Fig. S13. (a) Acidity or basicity of CH_3OH dispersed with P-DILsOH. (b) Acidity or basicity of CH_3OH dissolved with NaOH.

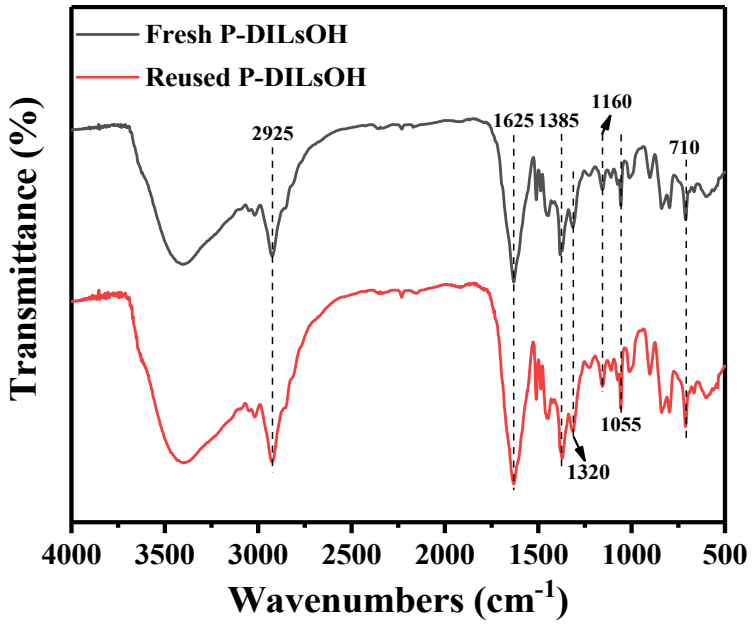

Fig. S14. FT-IR spectra of fresh and reused P-DILsOH.

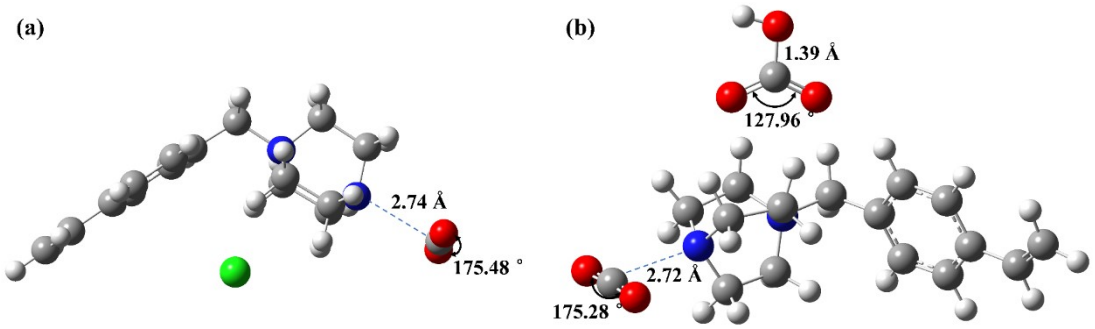

Fig. S15. Optimized structures of interaction between basic ILs monomers and CO_2. (a) [VBTEDA]Cl+CO_2, (b) [VBTEDA]OH+2CO_2.

Table S1. Textural parameters of LB-PILs.

PILs	S_{BET}[a] ($m^2 \cdot g^{-1}$)	V_P[b] ($cm^3 \cdot g^{-1}$)	D_{ave}[c] (nm)
P-IMCCl	59.85	0.1537	10.27
P-IMCOH	87.51	0.1986	9.08
P-BCACl	18.48	0.0275	5.96
P-DILsCl	15.68	0.0278	7.10
P-DILsOH	22.58	0.0570	10.09

[a] BET specific surface area. [b] Total pore volume. [c] Average pore size.

Table S2. Effect of CH_3OH addition timing on DMC yield in two-step coupling reaction.

Entry	Two-step coupling reaction		
	DMC Yield (%)	GLC Yield (%)	By-product Yield (%)[c]
1[a]	9	31	58
2[b]	77	20	Trace

[a] Reaction conditions: GO (15 mmol), CO_2 (10 bar) and CH_3OH (225 mmol) were added into the reaction system together (140 ^oC, 2.5 h, 100 mg P-DILsOH).

[b] Reaction conditions: CO_2 (10 bar) cycloaddition reaction with GO (15 mmol) were carried out at 80 ^oC for 1 h over P-DILsOH (100 mg). And then CH_3OH (225 mmol) was added into the reaction system (140 ^oC, 1.5 h, without CO_2).

[c] GO was alcoholized by CH_3OH.

Table S3. Catalytic performances about cycloaddition reaction of CO_2 with epoxides.

Catalysts	PC Yield (%)[a]	GLC Yield (%)[a]	CEC Yield (%)[b]	SC Yield (%)[c]
P-IMCCl	59	68	60	57
P-BCACl	84	85	82	80
P-DILsCl	73	76	71	69
P-DILsOH	96	97	94	92

[a] Synthetic condition: PO/GO 15 mmol, 80 °C, 10 bar CO_2, 1.0 h and 100 mg P-DILsOH.

[b] Synthetic condition: ECH 15 mmol, 100 °C, 10 bar CO_2, 1.0 h and 100 mg P-DILsOH.

[c] Synthetic condition: SO 15 mmol, 120 °C, 10 bar CO_2, 1.5 h and 100 mg P-DILsOH.

Table S4. Two-step synthesis of DMC by various epoxides.

Entry	Epoxides	Cycloaddition reaction[a]		Transesterification reaction[c]	
		GLC Sel. (%)	GLC Yield (%)	DMC Yield (%)	By-product Yield (%)[d]
1	PO	98	96	81	Trace
2	GO	98	97	77	Trace
3[b]	GO	99	10	Trace	28
4	ECH	99	94	68	Trace
5	SO	97	92	75	Trace

[a] The conditions of CO_2 cycloaddition reaction were consistent with those shown in Table S3.

[b] No catalyst was added.

[c] Reaction conditions: CH_3OH (225 mmol), 140 °C, without CO_2, 1.5 h.

[d] The remaining GO was alcoholized by CH_3OH.

Table S5. Comparison of the catalytic performances of different PILs catalysts for the cycloaddition reaction of CO_2 and SO to SC.

NO.	Catalyst	Reaction conditions	SC yield[a] (%)	Ref.
1	3-IPMP-EtI	SO (30 mmol), Cat. (150 mg), 1.0 MPa, 90 °C, 5 h.	88	4
2	PEAMCl	SO (10 mmol), Cat. (100 mg), 1.0 MPa, 120 °C, 4 h.	97	5
3	IHCP-OH (0.5)	SO (15 mmol), Cat. (5 μmol ionic sites), 3.0 MPa, 408 K, 2 h.	94	6
4	PAD-3	SO (5 mmol), Cat. (100 mg), 1.0 MPa, 110 °C, 0.5 h.	90	7
5	NHC-CAP-1 (Zn^{2+})	SO (41.5 mmol), Cat. (25 mg, 1.61 wt% of Zn), 2.0 MPa, 100 °C, 3 h.	81	8
6	P-[EEBVIM]Cl_2-EGDMA	SO (5 mmol), Cat. (2 mg), 1.0 MPa, 100 °C, 96 h.	95	9
7	P-DILsOH	SO (15 mmol), Cat. (100 mg), 1.0 MPa, 120 °C, 1.5 h.	92	This work

[a] Cycloaddition activity of SO with CO_2 reported in the references.

Table S6. Comparison of the catalytic performances of different types of catalysts for two-step synthesis of carbonates.

NO.	Catalyst	Reaction conditions	Carbonates yield[a] (%)	Ref.
1	K_2CO_3/$BrBu_3PPEG6000PBu_3Br$	Cycloaddition: PO 14.3 mmol, Cat. 1.1344 g, 1 MPa, 120 °C, 6 h.	PC: 99 %	10
		Transesterification: alcohol 430 mmol. 100 °C, 1.5 h.	DMC: 99 % DEC: 72 %	
2	MCM-41-pr-$TMEDA^+Cl^-$	Cycloaddition: PO 30 mmol, Cat. 132 mg, 2 MPa, 120 °C, 6 h.	PC: 99 %	11
		Transesterification: CH_3OH 750 mmol. 120 °C, 4 h.	DMC: 68 %	
3	KI/K_2CO_3	Cycloaddition: EO 200 mmol, Cat. I 3.76 mmol, Cat. II 0.9 mmol, 2.5 MPa, 120 °C, 1 h.	EC: 99 %	12
		Transesterification: CH_3OH 1125 mmol. 60 °C, 0.5 h.	DMC: 82%	
4	P-DVB-AEImIm	Cycloaddition: GO 15 mmol, Cat. 100 mmol, 1 MPa, 80 °C, 1 h.	GLC: 97 %	This work
		Transesterification: alcohol 225 mmol. 140 °C, 1.5 h.	DMC: 77% DEC: 73% DPC: 67%	

[a] Catalytic activity of two-step synthesis of carbonates with CO_2, epoxide and alcohols as raw materials in the references.

Table S7. Comparison of cycloaddition activities over P-DILsOH and KBr under different reaction conditions.

Entry	Catalysts	Cycloaddition reaction	
		Selectivity (%)	Yield (%)
1[a]	P-DILsOH	98	97
2[b]	KBr	99	95

[a] Reaction conditions: GO (15 mmol), 80 °C, CO_2 (10 bar), 1 h, P-DILsOH (100 mg).

[b] Reaction conditions: GO (15 mmol), 110 °C, CO_2 (20 bar), 2 h, KBr (100 mg).

Table S8. Two-step synthesis of DMC over various catalysts.

Entry	Catalysts	Cycloaddition reaction[a]		Transesterification reaction[b]	
		GLC Sel. (%)	GLC Yield (%)	DMC Yield (%)	By-product Yield (%)[d]
1	P-DILsOH	98	97	77	Trace
2	KBr	99	62	Trace	24
3	NaOH	97	71	56	23
4[c]	KBr/NaOH	98	64	49	30

[a] Reaction conditions: GO (15 mmol), 80 °C, CO_2 (10 bar), 1 h, catalysts (100 mg).

[b] Reaction conditions: CH_3OH (225 mmol), 140 °C, without CO_2, 1.5 h.

[c] Binary catalysts: KBr (50 mg)/NaOH (50 mg).

[d] The remaining GO was alcoholized by CH_3OH.

REFERENCES

[1] J. B. Huang, C. He, L. Q. Wu, H. Tong, *J. Energy Inst.,* 2017, **90**, 372-381.

[2] T. Lu, F. W. Chen, *J. Comput. Chem.*, 2012, **33**, 580-592.

[3] W. Humphrey, A. Dalke, K. Schulten, *J. Mol. Graphics*, 1996, **14**, 33-38.

[4] W. Zhang, Y. Mei, P. Wu, H. H. Wu, M. Y. He, *Catal. Sci. Technol.*, 2019, **9**, 1030-1038.

[5] X. C. Wang, Q. Dong, Z. Z. Xu, Y. Wu, D. M. Gao, Y. S. Xu, C. J. Ye, Y. T. Wen, A. Q. Liu, Z. Y. Long, G. J. Chen, *Chem. Eng. J.*, 2021, **403**, 126460.

[6] D. G. Jia, L. Ma, Y. Wang, W. L. Zhang, J. Li, Y. Zhou, J. Wang, *Chem. Eng. J.*, 2020, **390**, 124652.

[7] Z. J. Guo, X. C. Cai, J. Y. Xie, X. C. Wang, Y. Zhou, J. Wang, *ACS Appl. Mater. Interfaces*, 2016, **8**, 12812-12821.

[8] P. Puthiaraj, S. Ravi, K. Yu, W. S. Ahn, *Appl. Catal. B: Environ.*, 2019, **251**, 195-205.

[9] H. B. Song, Y. J. Wang, M. Xiao, L. Liu, Y. L. Liu, X. F. Liu, H. J. Gai, *ACS Sustainable Chem. Eng.*, 2019, **7**, 9489-9497.

[10] J. S. Tian, C. X. Miao, J. Q. Wang, F. Cai, Y. Du, Y. Zhao, L. N. He, *Green Chem.*, 2007, **9**, 566-571.

[11] J. Li, L. G. Wang, S. M. Liu, X. L. Li, F. Shi, Y. Q. Deng, *Chem. Lett.*, 2010, **39**, 1277-1278.

[12] J. Q. Wang, J. Sun, C. Y. Shi, W. G. Cheng, X. P. Zhang, S. J. Zhang, *Green Chem.*, 2011, **13**, 3213-3217.

[13]